Global Scientific JOURNALS

GSJ: Volume 9, Issue 4, April 2021, Online: ISSN 2320-9186

www.globalscientificjournal.com

The effect of "CTR" frequency on the optoelectronic - energy conversion efficiency for smart new generation device

Zeinab ELSayed ELMANDOUH[1], Hesham Azmi ELMELEEGI[1],Gehan Mahmoud ELKOMI[1], Isaad Mohy-ELDIN [1]

[1:] Electron Microscope and Thin Films Department, Physical Research Division,National Research Center, Dokki, Cairo, Egypt , Aff. ID: 60014618

1. Abstract

AC conductivity was studied to characterize the behavior of $Ge_{20}Bi_xSe_{80-x}$ composition and to decide the best composition for building higher efficiency solar cell. Correlated barrier hopping mechanism of conduction is dominant. The solar cell prepared from p-type; $Ge_{20}Bi_5Se_{75}$ and n-type $Ge_{20}Bi_{15}Se_{65}$ has been studied. Chalcogenides of such device was prepared by melt quenching technique. Carrier – Type Reversal (CTR) phenomenon was elucidated to have fascinating effect on optoelectronic energy conversion efficiency. The energy conversion efficiency was found to be around 9%. Characterizing solar cell by current-voltage curve, open circuit voltage V_{oc}, short circuit current I_{sc} and Fill Factor. A recent applicable characteristics of this junction is its ability to act as a memristor .

$Ge_{20}Bi_xSe_{80-x}$, X = 0.5 and 0.15 % is a harvesting device for distinguished applications as a solar cell and as a memristor.

Key Words:

Solar Cell- Memristor- smart multipurpose device- Carrier Type Reversal- Chalcogenide Thin Films.

1. Introduction:

Germanium chalcogenide glassy alloys have excellent role in both; electronic and optoelectronic applications. The structural model describing Ge-Se glasses is based upon the Ge atoms with coordination four and selenium atoms via coordination two [(1)].Amorphous chalcogenide glasses prepared by melt-quenching generally behave as p-type conduction as evidenced by thermoelectric power measurements [(2)]. The phenomenon of carrier - type reversal was achieved by Bi or Pb addition into Ge-based chalcogenide glasses with a certain atomic percentage [(3)]. CTR has been attributed[(4)] to the pinning of the Fermi level towards the conduction band due to the upset of the equilibrium between negatively D^- and positively D^+ charged defect states.[(5)]

A study of the electrical and optical properties of amorphous Ge_{20} M_{75} Bi_5(M=S, Se or Te) was investigated. The Fermi level was shifted from the mid gap due to the unbalance in C^- and C^+ charged centers. Incorporation of 5 at% Bi seems to have no drastic effect on the electronic structure as the Fermi level is still pinned at midpoint[(6)],[(7)] The electrical resistivity of $Ge_{20}Bi_xSe_{80-x}$ glasses with (x= 0 to 25)were measured. The electrical activation energy of the films was determined by investigating

the temperature dependence of, resistivity. A large decrease in the electric activation energy was observed as Bi content was increased up to 10 at %. The optical and electrical data explained that the addition of Bi produces localized states near the edge of conduction band. Increasing the Bi content decreases the activation energy. So, the expected transport properties is due to electrons hopping caused by excitation into localized states at the conduction band edge. The melt quenched chalcogenide glasses are p-type semiconductors and unlike crystalline semiconductors it is difficult to change the type of conductivity by doping. According to the charged dangling bond model [8-11], the insensitivity of these chalcogenide glasses to impurities is ascribed to the presence of negatively charged dangling bonds, which pin the Fermi energy level[12].The incorporation of Bi into Ge-Se glasses brings a reverse conduction type from p- to-n. AC-conductivity of $Ge_{20}Bi_xSe_{80-x}$ thin film samples has been measured as a function of frequency and temperature. The most suitable theoretical model that can describe the mechanism of conduction was the correlated barrier hopping one[13].

2. Experimental technique

Bulk samples of $Ge_{20}Bi_xSe_{80-x}$(x=5,15) were prepared by melt quenching technique. High purity (99.999%) elements with appropriate atomic percentage were sealed in silica ampoule in vacuum. The ampoule was kept in furnace for 24 hour at 1100 C^o. Thin 'films of various compositions of $Ge_{20}Bi_xSe_{80-x}$were prepared by thermal evaporation technique. The lack of crystallinity of the samples was confirmed by the absence of any sharp peak in the x-ray diffraction pattern. The

thickness and the surface morphology of the prepared thin films were measured by High Resolution field emission scanning electron Microscope (HRFESEM), Quanta 250., The electrical measurements was done by Keithley 6517A electrometer .

4. Results and discussion:

4.1 A.C. Conduction Measurements

The experimental results of ac conductivity (σ_{ac}) are usually expressed by the following relation:

$(\sigma_{ac}) = \sigma_{ac}(0) + \sigma_{ac}(w)$……..4.1

Where $\sigma_{ac}(0)$ is the de-conductivity of the sample and σ_{ac} (w) is the frequency dependent component of the conductivity, which was typically expressed by the power law:

$\sigma_{ac}(w) = A\sigma w^n$ describing the conduction carried on by hopping mechanism of charge carriers [14].

The suitable theoretical model that can describe the function σ_{ac} *(w)* was the correlated barrier hopping (CBH) model [15]. In this model the current carriers hop between sites over a coulombic barrier of height W of magnitude.

$$W = w_m - \left(\frac{n_e e^2}{\pi\varepsilon\varepsilon_0 r}\right) \quad \text{..... (4.2)}$$

where W_m is the maximum barrier height for hopping, r is the separation between two hopping sites, e is the electronic charge, ε: is the permittivity of the sample, and n_{el} is the number of simultaneously hopped carriers between centers (n_{el} = 1or 2) for a single or bipolaron transport, respectively [16].

The ac conductivity of $Ge_{2o}\ Bi_x\ Se_{80-x}$ (where x = 5 and 15) has been measured as a function of frequency and temperature and represented in Fig (4.1and 4.2). The experimental work reveals that σ_{ac} increases with increasing temperature from 303K to 383K especially in the range from DC frequency to 2MHz . Effect of Bi on conductivity indicate that Bi= 5 at. % has the highest value of conductivity and σ_{ac} decrease with increasing Bi

dopant; that increasing will affect the distribution of valence and conduction band. Since increasing (Bi) doping increases defect states in conduction band and facilitate the motion of electrons and hole so σ_{ac} increases. The increase of applied frequency enhances the electronic jumps between the localized states consequently increasing ac conduction providing evidence for the existence of hopping type conduction mechanism [17].

For calculating capacitance equation (4-3) could be applied [18]

$$C = C_o + \frac{1}{w^2 R^2 C_o} \quad \ldots\ldots\ldots\ldots\ldots\ldots\ldots\ldots\ldots\ldots\ldots\ldots\ldots\ldots(4.3)$$

Where: w is the the angular. frequency. R is the resistance, Co is the frequency independent capacitance. Fig (4.3,4.4) represents the variation of capacitance with frequency at various temperatures. The figure shows that at high frequencies the 'capacitance for all temperature converges towards single value to demonstrate that the

capacitance may become temperature independent.

The drastic increase of capacitance in the high frequency range at the high temperatures is probably due to space charge polarization induced by increasing number of free charge carrier as a result of increasing temperature. The capacitance was increasing as increasing Bi dopant.

When the frequency of alternating voltage increases the value of ε of a polar dielectric at first remains invariable but at certain critical frequency, and when polarization fails to settle itself completely ε begins to drop approaching at very high frequencies the values typical of nonpolar dielectrics. This is confirmed by the data in the Fig.(4.5,4.6) which represent the relation between ε'1 as function of frequency and temperature.

The dielectric constant

$$\varepsilon' = C/Co \ldots\ldots\ldots\ldots\ldots\ldots\ldots\ldots\ldots\ldots\ldots\ldots(4.4)$$

Relaxation time is given by

$$\tau_d = \frac{\varepsilon}{\sigma} = \rho\, \varepsilon \quad \ldots\ldots\ldots\ldots\ldots\ldots\ldots\ldots\ldots\ldots\ldots\ldots\ldots\ldots(4.5)$$

Where Where σ is the electric conductivity, which is a measure of the concentration and the mobility of variable mobile carriers, and ε is the permittivity, which is a measure of the strength of the coulombic interaction inside the semiconductor (the dielectric medium).

Thus, the product ρ ε can be thought of as the RC (R is the resistance and C is the capacitance) time constant of the materials. Obviously, the larger the value of τ_d is, the longer the time required to attain equilibrium [19]

The graph between τ(relaxation time) as a function of frequency and temperature Fig (4.7,4.8) shows a decrease of τ with increasing frequency for all concentration The maximum value of τ was for sample Ge_{20} Bi_5 Se_{75}.

The Loss Tangent (tan δ):Many relaxation processes have· been considered by different authors and for each relaxation process one can suppose that the spectrum of relaxation time is rather wide and flat in amorphous materials.

When a semiconductor is subjected to an ac voltage the current lags by 90°. However in a regular dielectric the lag is not 90° but (90° - θ*)* where θ is the phase angle then δ= (90°- θ*)*, where δ is called the dielectric loss angle and this behavior leads to a power loss generally as heat. To minimize the energy dissipation from a given material, one must seek for the lowest value of δ.

However, loss tangent **(tan** δ) is equal to:

$$\text{Tan } \delta = \frac{\varepsilon''}{\varepsilon'} \quad \text{..... 4.6}$$

Where ε'' is imaginary part of dielectric constant and ε' is the real part of dielectric costant.

Fig(4.9,4.10) show a set of curves for dependence of tanδ on temperature and frequency for Ge_{20} Bi_x Se_{80-x} with *(x=5,and,*15 at.%). An anomalous displacement of the maxima to higher frequency with increasing Bismuth content

By comparing the relation between tan δ and frequency for two composition of $Ge_{2o}Bi_xGe_{80x}$ where x=5, and 15, it was clear that sample $Ge_{20}Bi_{15}Se_{65}$ is better for application since it has the lowest loss tangent tan *δ.*

A.C.conductivity measurements have been widely used to investigate the nature of defect centers in chalcogenide glasses since it is assumed that they are responsible for the type of conduction. Elliot[(20)] proposed that CBH (correlated barrier hopping) model which is based on the concept of charged defect states D+, D- in chalcogenide glasses which is responsible for conduction. It is assumed that for most of the materials at low to

intermediate temperatures, only charged defect centers are present, i.e., the effective correlation energy U_{eff} is sufficiently large ($U_{eff} >> K_BT$) such that all neutral D^0 centers are converted to D+ and D- centers in this case if an alternating field is applied, the simultaneous motion of two electrons is the only possible form of electron· transfer between that preserves the identity of the defects. In the intermediate temperature regime, the CBH mechanism involving bipolaron transport gives a satisfactory description of the experimental data in most of the amorphous alloys.(21)

4.2. Chacogenide Device as a solar cell:

The sketch of the cell is shown in Graph (1). The amorphous structure is the main reason for tailing and extending the band edges(22). In the amorphous structure, both weak and strained dangling bonds, and defect-impurity can give rise to the formation of states in the gap. The net effect is a distribution of states in the mobility gap(23). The performance of the solar cell depends on the cross- section capturing of both levels in the charged and the neutral states. A typical current-voltage characteristic of a solar cell under illumination is shown in Graph(2). The following parameters define the performance of the cell; the open-circuit voltage (V_{oc})and, the short- circuit current (I_{sc}) and Fill Factor (FF).The Fill Factor can be calculated from the following equation;

$$Fill\ factor = \frac{I_{max} \times V_{max}}{V_{oc} \times I_{sc}} \qquad (4.1)$$

Where $V_{max}$and I_{max} are the values of the voltage and the current obtained under illumination when I_{sc}=0 and V_{oc}=0 respectively.

The Energy conversion efficiency of the cell(24)

$$\eta = \frac{power\ \ output}{power\ \ input} \qquad (4.2)$$

Where:-

7

$$\eta = \frac{V_{oc} \times I_{sc} \times FF}{I \times A} \quad (4.3)$$

Where I is the intensity of the incident light in w/m^2, A is the solar cell area. TheI-V that characterize Ge- Bi-Se, system, solar cell in the day light can be illustrated in Graph(3). The parameters characteristics were listed in table[1].

Table [1]: Solar Cell Characteristics

V_{oc}	I_{sc}	V_{max}	Imax	Efficiency
0.75 V	8.60×10^{-5}A	0.35 V	4.10×10^{-5} A	9.2%

The efficiency of the prepared solar cell calculated from equation (3)was 9.2 % and this is a good result since the power injected to the cell was 1.5 watt/m^2which is a very low light power. The cell mentioned in this study needs more experimental treatments to improve the efficiency. Pattern of solar cell surface was taken by Field Emission HR Scanning Electron Microscope is presented in Plate (1). It shows homogeneous structure with embedded particles among the film material. The thicknesses of samples under investigation were estimated by Scanning E.M which revealed as 190 nm for n-layer while; 226 nm for p- layer. Spectrum analyzer used to analyze data from oscilloscope.

4.2 Recording the (CTR) Phenomenon in the Alternative Current Range:

A very fascinating experiment was done to elucidate the (CRT) in the system ($Ge_{20}Bi_xSe_{80-x}$) thin films shape from x=5%

8

to 15%. For determining the conduction type through the circuit which was reported in the experimental technique. Oscilloscope record, for Ge_{20} Bi_5Se_{75} thin film fresh sample, shows a negative left horizontal part represents the output from the specimen "of the input negative half cycle of the sine wave from function generator" which indicates an n-type conduction with a vertical downward represents the output of the positive half cycle part, inputted by the function generator, which indicates a p-type conduction at frequency 75.5 Hz.

Oscilloscope record for wave function for sample Ge_{20} $Bi_{10}Se_{70}$ represents a transition of majority carrier's type from n-type during forward half cycle to p-type during reverse half cycle at frequency 200 Hz as represented in Fig.(4-a,b,c). This phenomenon may be explained by **Mott**[25] concept of the disordered materials where the effect of an applied field from function generator on specimen is to modify the energy of a hop between the two states separated by a distance R by an amount eFRcosθ while θ is the angle between the direction of vector $\overleftarrow{F}$and$\overleftarrow{R}$and *e*is the electron charge 1.6 x 10^{-19} coulomb.

The conductivity is given by [25]:

$$\sigma = \sigma_e + \sigma_n = e^{(eFRcos\theta\ /KT)} \quad (4.4)$$

Whenθ = 0^o then cos θ= 1 which implies a coincidence both direction of $\overleftarrow{F}$and$\overleftarrow{R}$, in the reverse direction of charge carrier motion then θ = 180^o so cosθ = -1.

This system Ge_{20} Bi_xSe_{80-x} of thin film has a very good application as a new generation of a cheap and higher forward current value for a new P-N Junction and other electronic chips utilizing such mechanism (CTR).

9

Increasing Bi dopant to 15% at wt. the phenomenon of CTR disappeared due to increasing defect states in conduction band.

4.3 - Chalcogenide device as a"memristor"

The current-voltage characteristic of typical threshold switch[17]is shown in Graph (3)as butterfly pattern which indicates a good ferroelectric characteristics of BiGeSe .Graph (3) represents an off state, and at point (a)threshold voltage, the current increases sharply to the value(b) in the forward bias. While; the investigated thin films show an off state at a point (d) and an on state(c), both in the reverse bias. This switching device has a stable structure and does not exhibit a reversible change between amorphous and crystalline state. Such switching is a field assisted transition which makes the amorphous semiconductor switches from a highly resistance values to a conductive state at threshold voltage (V_{th}). A positive threshold ($+V_{th}$) causes high to low resistance transition and ($-V_{th}$) negative threshold voltage causes low to high resistance transition[18,19]. This system could be applied as a memristance according to equation[20]:

$$M\big(q(t)\big) = R_{off} - \left[1 - \frac{M_{\upsilon} R_{on}}{D_2} q(t)\right] \qquad (4.5)$$

$R_{off}$is the high resistance state, R_{on} represents the low resistance state, M_{υ}:mobility of dopants, and D represents the film thickness. The switching behavior itself is clearly observed as a property of PRAM (Programmable Random Access Memory) mechanism as

revealed in Graph(3). Various models have been proposed, e.g.; those based on trap-controlled, space-charge-limited current[21], defect states inside the band gap and electric-pulse-induced motion [22-25]. However; the chalcogenides are promising and versatile as they exhibit more than one type of industrial application and a new generation of smart devices that plays a multi - functional uses.

Conclusion:

A solar cell was prepared from p-type: $Ge_{20}Bi_{15}Se_{75}$ and, n-type: Ge_{20} $Bi_{15}Se_{65}$. The efficiency of the cell studied in this research was found to be around 9% for most of the samples under weak illumination. The cell surface was homogenous as confirmed by HRSEM. The parameters of the solar cell are the values of V_{oc}= 0.5v, I_{sc}= $8.6*10^{-5}$A while V_{max}=0.35 volt and I_{max}= $4.1*10^{-5}$A. Another application was observed for such device which is switching. The device could be applied as a memoristor since there are two states the off state is (ad), whereas the on state can be the upper part of the curve (bc).

References

1. Trone, P.; Bensoussan, M.; Brenace, A. *Phys. Rev. B.* 1973, 8, 5947.

2. Frumar, M.; Tichy, L. *J. noncryst. Solids*1987, 97/98, 1139.

3. Tonge, N.; Minami, T.; Tanaka, M. *J. Noncryst. Sol.* 1980, 37, 23.

4. Tohge, N.; Matsuo, H.; Tanaka, M. *J. Noncryst. Sol.*1985, 96, 809.

5. Tohge, N.; Minami, T.; Tanaka, M. *J. Noncryst. Sol.*1980, 38/39, 283.

6. Ortiz- Conde, A.; Garcia Sauchez, F. J; . Muci, *J.Solar Energy Mater Solar*

Cells, 2006, 90, 352.

7. Kaminsk, A.;Mavchand, J. J.; Laugier, A. *Solar Energy Mater. Solar Cells*,

1998 ,51,221.

8. Van. Roosbroeck, W.; Casey,H. C. *J Phys. Rev.***1972,** B5, 2154.

9. Kolomiets, B. T. *Phys. Status. Solidi*. **1968**,7,359.

10. Dohler, G. H.; Heyszenau, H.; *Phys. Rev. Lett.***1973**,30,1200.

11. Ashrey,A.; Farag, A.; Mahani,R.*Microelectronic Engineering*

2010,87,2218.

12. Toghe, N.; Kanda, K.;Minami,J.*Appl. Phys. Lett.***1986**,48,1739.

13.Averyanov,V.L.;Gelmoni,B.L;Kolmiets,B,T.;Lyubin,V,M;
Prikhodco,O.Yu.;Tsendin,K.D.J.Non-Cryst Solids (1984)64,279.

14..Chen.X, Wu N; J.strozier and Igntiev
A.,Appl.Phys.Lett.89,(2006),063507

15. Ignatier, A. , Wu, N.J.; Chen, X.; Liu SQ, C.Papagianni and J.Strozier. Phys. Status Solidi B 243(2006)2089.

16. K.L.Chopra., J.Appl.Phys.36,(1965),184.

17.Beck.A.,J.G.Bednorz, Ch.Gerber,C.Rossel,and D.Widmer, Appl.Phys.Lett.77,(2000),139.

18.Chen.X., Wu.N.,J.Strozier, And, Ignatiev A., Appl.Phys.Lett.89,(2006),063507.

19.Marshal J. M.,and,A.E.Owen.,Phyl.Mg.24(1971)1281.

20.Elliott,S.R.,Adv.Phys.36(1987)135.

21.Chndel.N.,Meht.N.,Kumar.N.A.,Current.AAa.Phys.(2012)12,405.

22. Ananth R.T.; ChithraLekha, P. ; Sanjeeviraja, C; Sanjeevinaja, D.P; athinattam P.,J.Non.Cryst. Sol. **2014** 405, pp21-26.

23. Vshinsky,SO; *phys. Rev. lett.*21,**1968**, 1450.

24. Katyal, S.;Kano,S.; Bando,T.;Suzuki,M.; *J. Non. Cryst. Sol.***1987**,97,779.

25. Mott,N.F.; Davis,E.A;Street,R.A. Pylos.Mag.B1975,32,96.

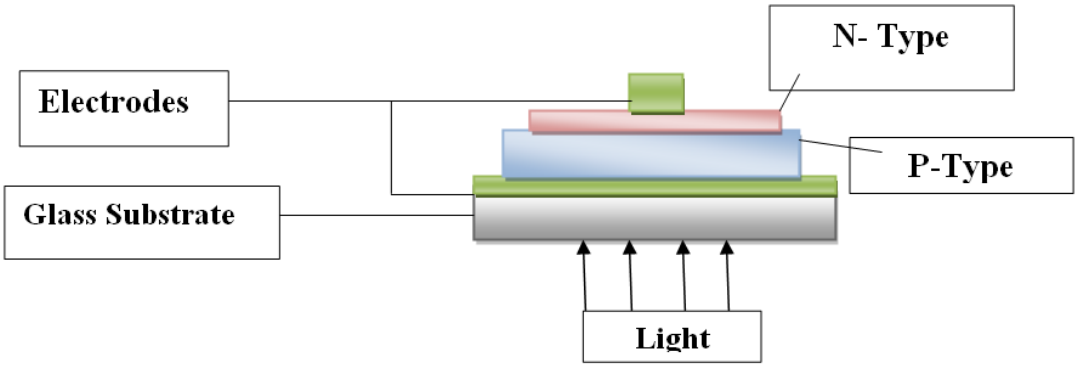

Graph [4.1]: The sketch of the cell.

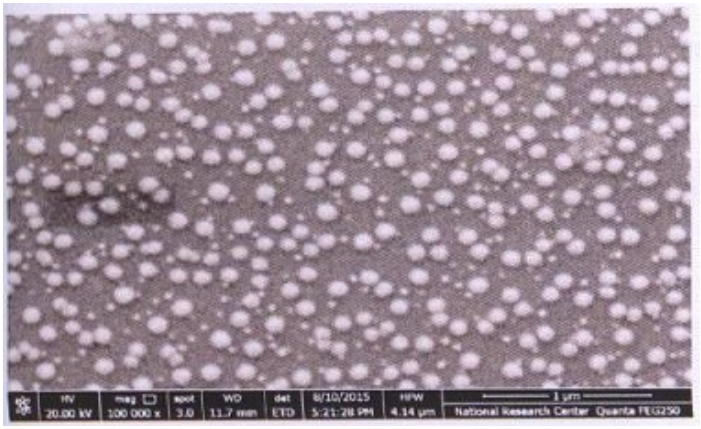

Plate [4.2] : Scanning Electron Microscope Of The Cell Surface.

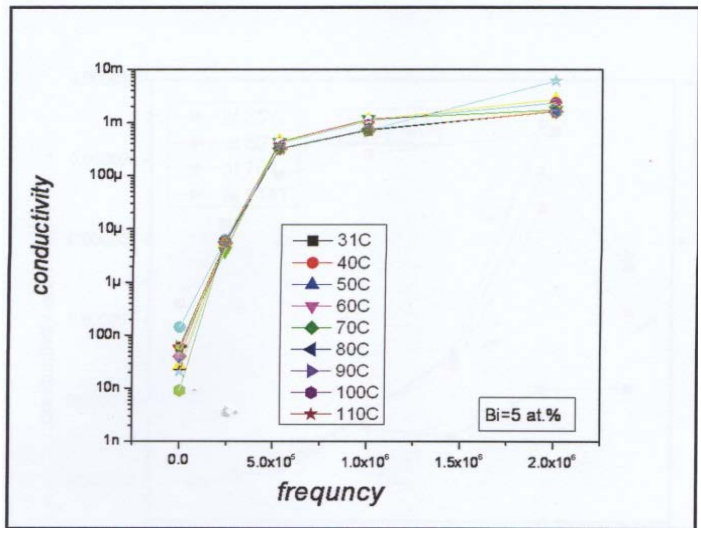

Fig. [4.1]

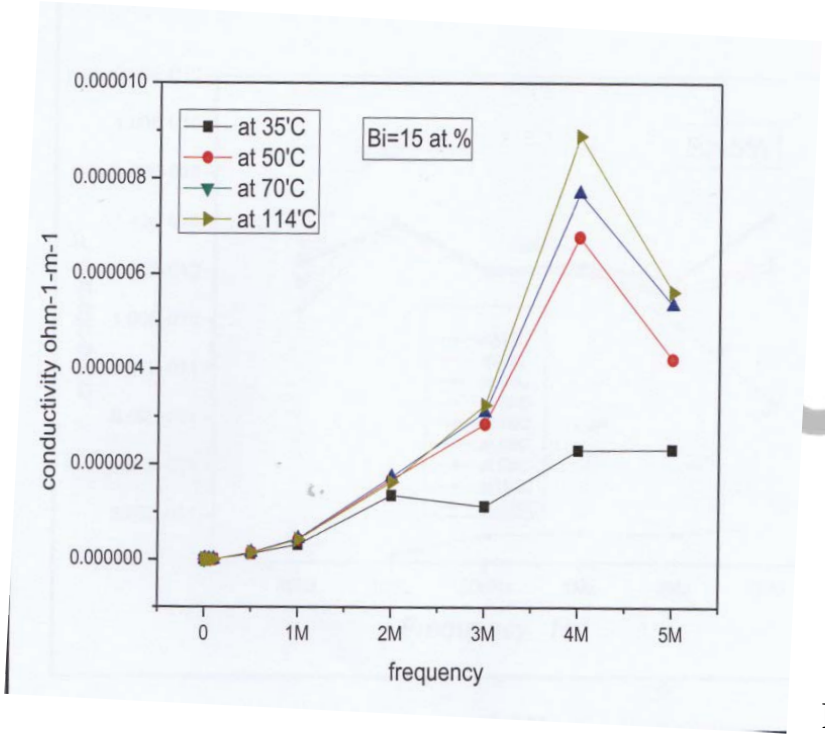

Fig.[4.2]

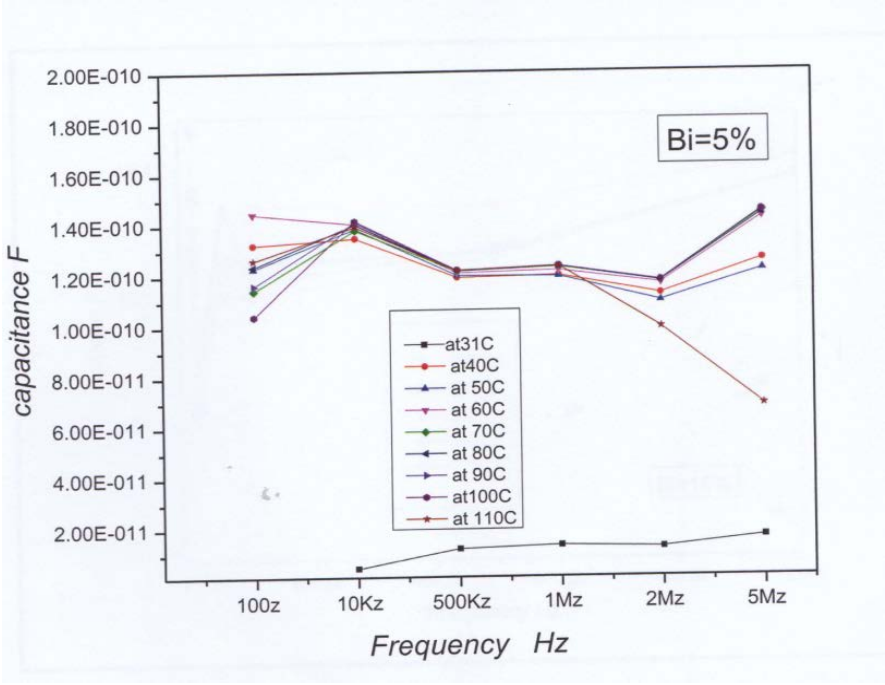

Fig.[4.3]

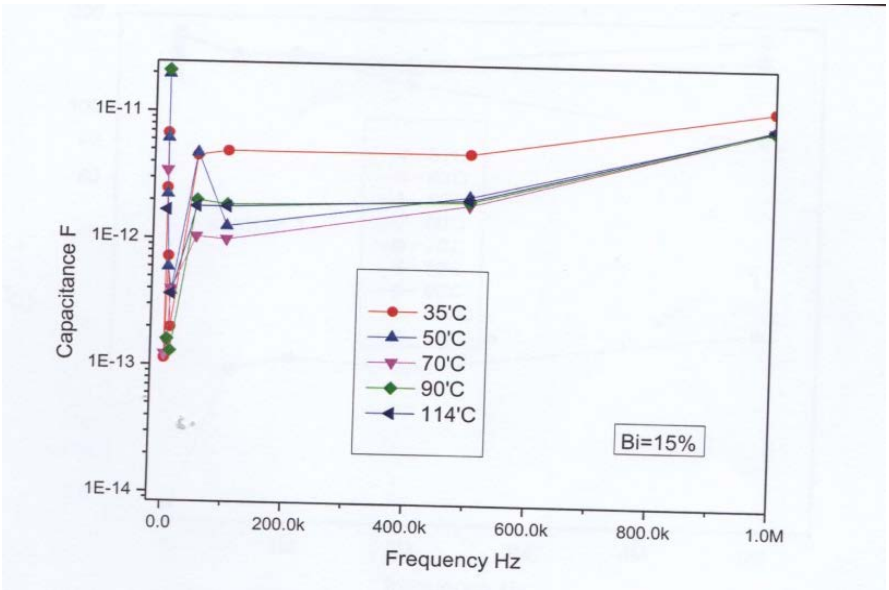

Fig.[4.4]

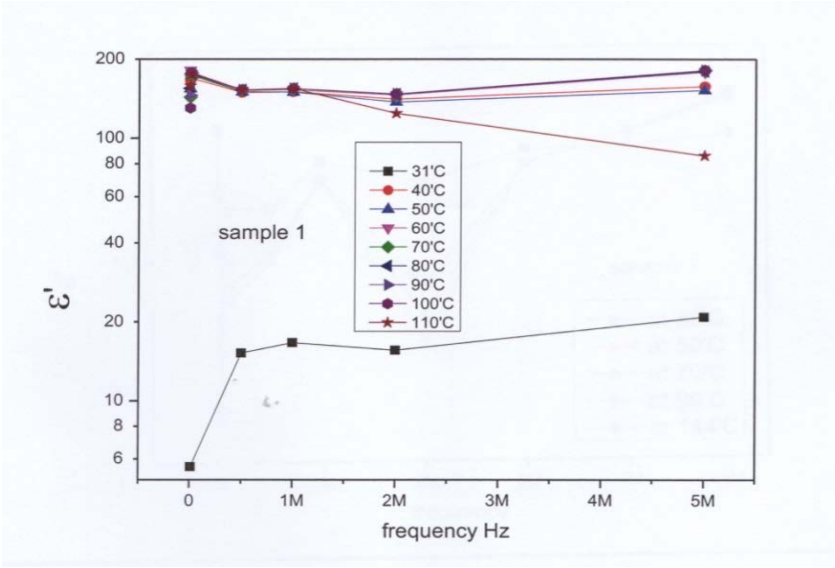

Fig.[4.5]

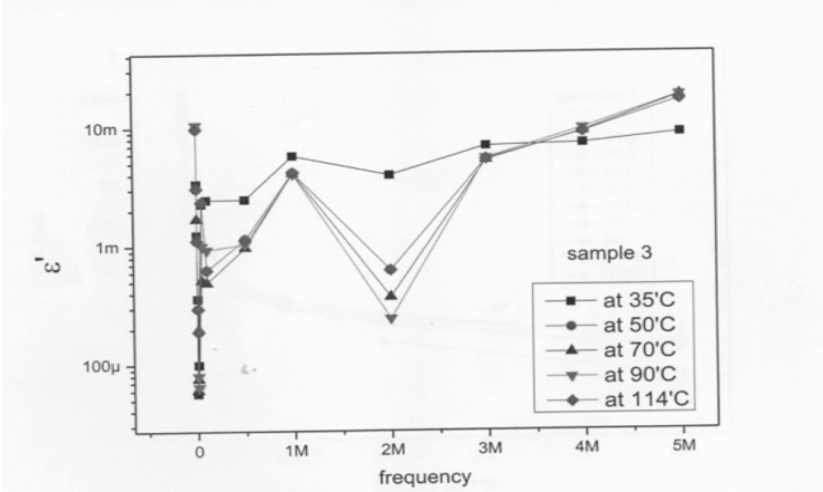

Fig[4.6]

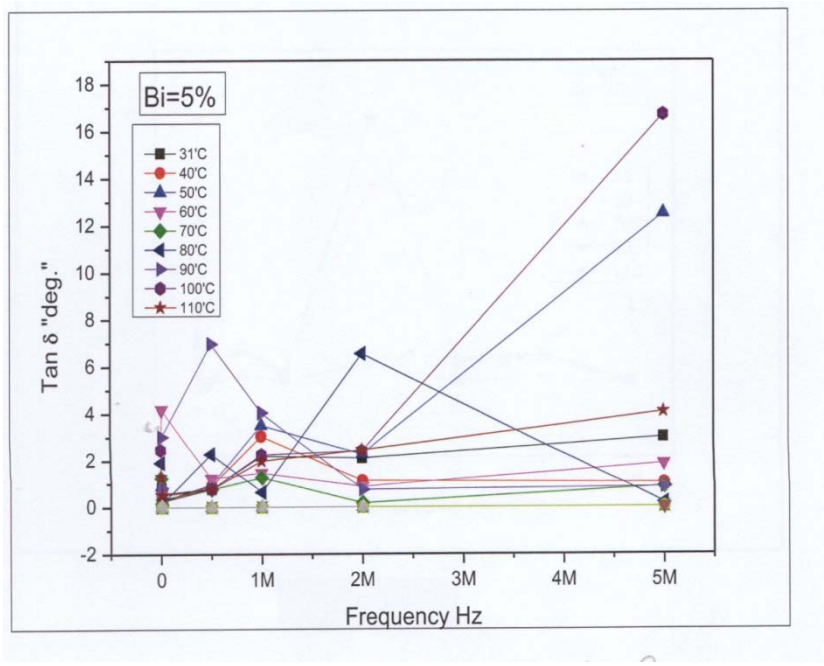

FIG.[4.9]

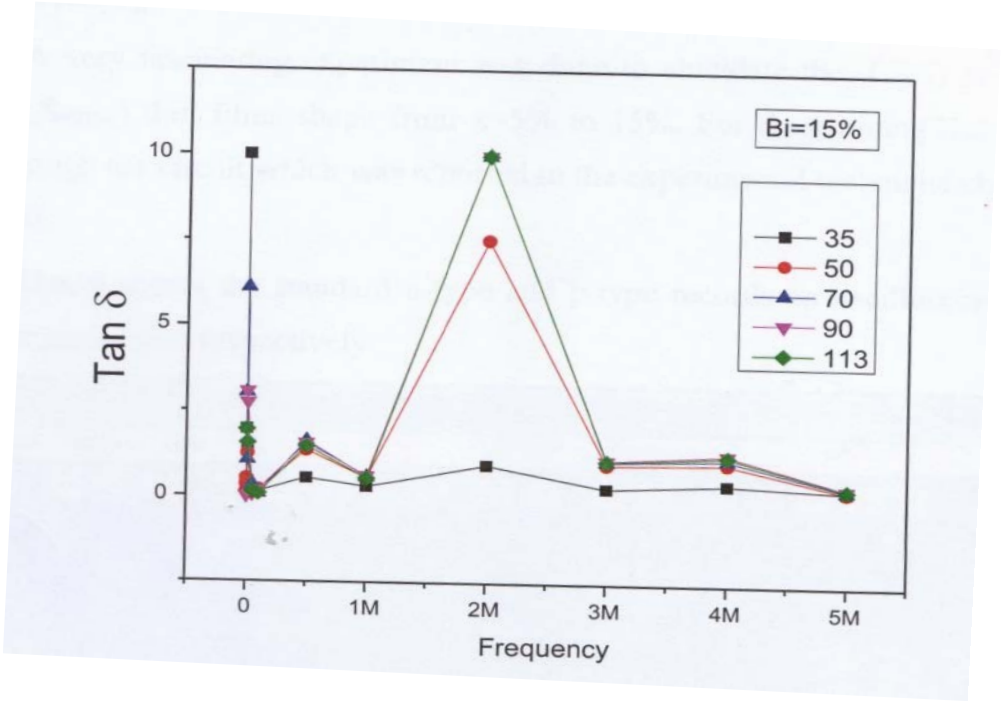

Fig.[4.10]

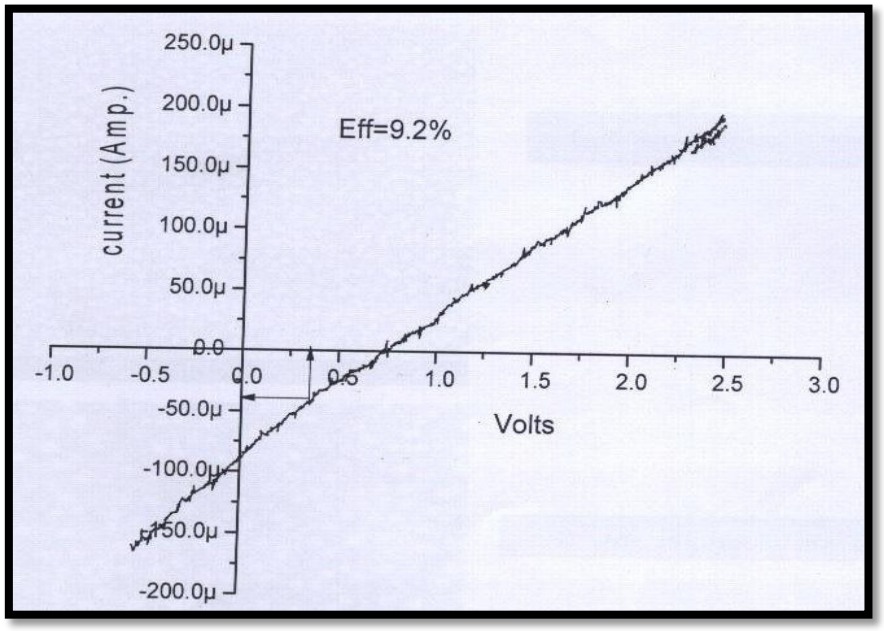

Graph (4.3): a typical relation between current and voltage of a solar cell as a characteristic for pn junction of GeBiSe a- thin film sample

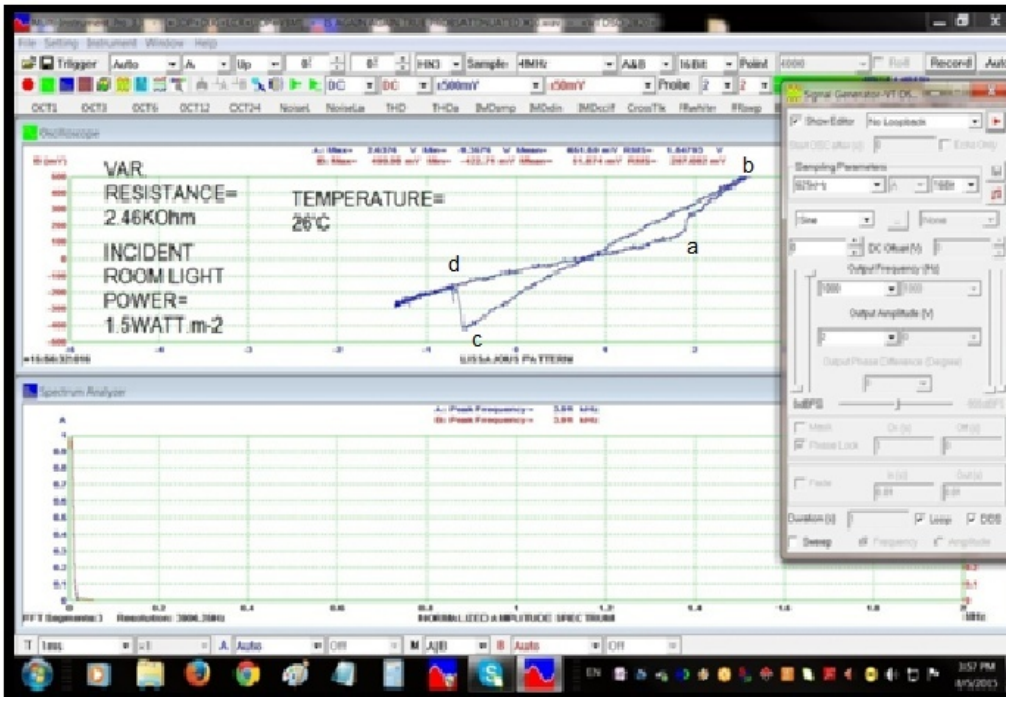

Graph(4.4): memristor I-V curve "Butterfly in shape"

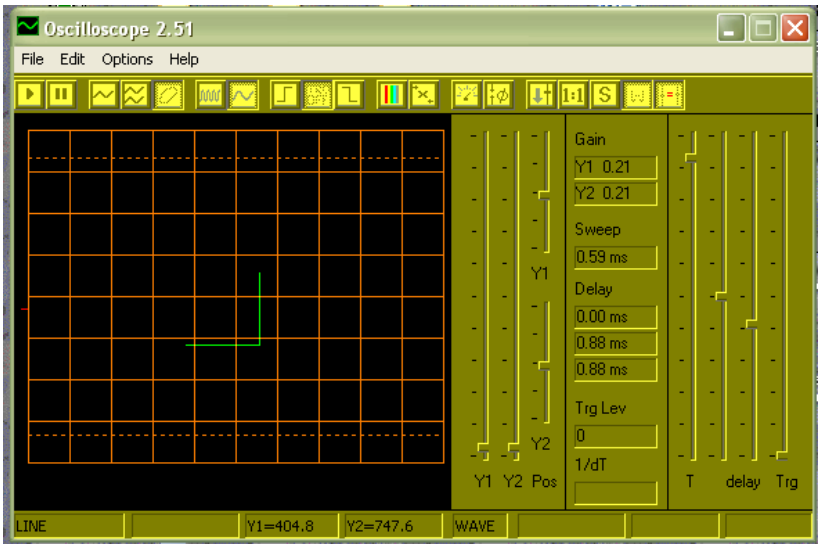

Figure 4.5.a : N-Type Material

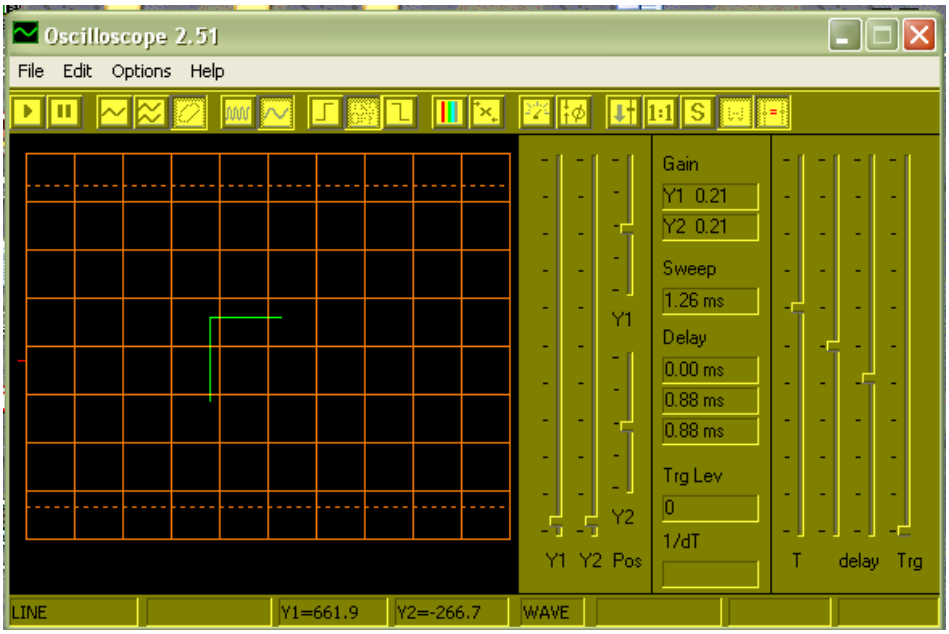

Figure 4.5.b : P-Type Material.

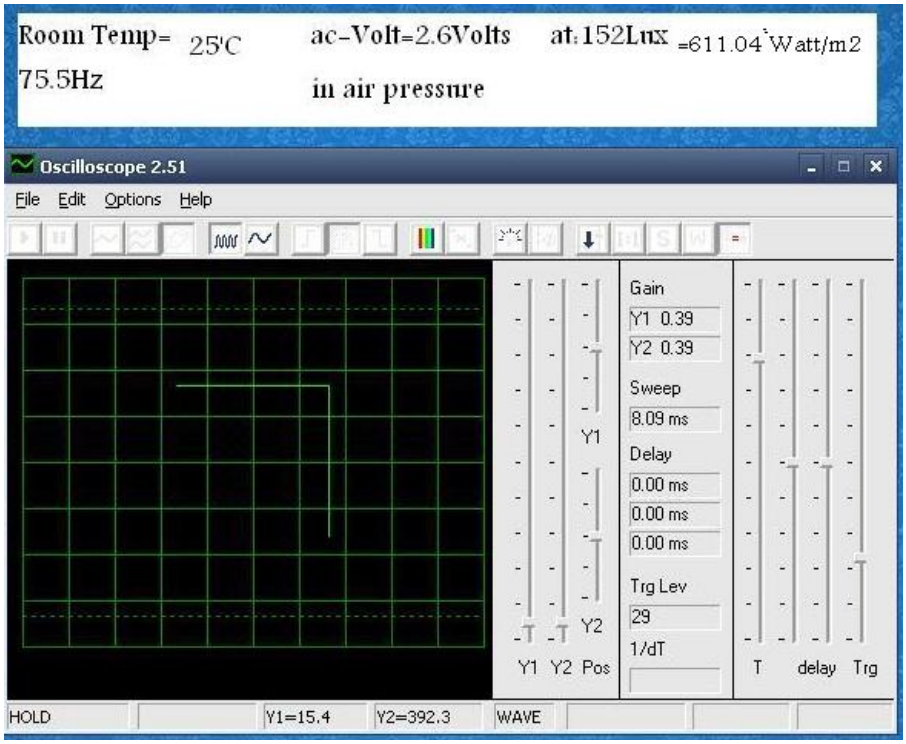

Figure 4.5.C : This is a P / N Transition Taken Upon Investigating One Of Layers That Can Form P/N Junction.